Hierarchical gradient of timescales in the mammalian forebrain

Min Song[1,14], Eun Ju Shin[2,3,14], Hyojung Seo[4,5,6], Alireza Soltani[7], Nicholas A. Steinmetz[8], Daeyeol Lee[9,10,11,12]*, Min Whan Jung[2,3]*, and Se-Bum Paik[13]*

[1] Department of Bio and Brain Engineering, Korea Advanced Institute of Science and Technology, Daejeon 34141, Republic of Korea.

[2] Department of Biological Sciences, Korea Advanced Institute of Science and Technology, Daejeon 34141, Republic of Korea.

[3] Center for Synaptic Brain Dysfunctions, Institute for Basic Science, Daejeon 34141, Republic of Korea.

[4] Interdepartmental Neuroscience Program, Yale University, New Haven, CT 06520, USA.

[5] Department of Psychiatry, Yale University, New Haven, CT 06520, USA.

[6] Department of Neuroscience, Yale University, New Haven, CT 06520, USA.

[7] Department of Psychological and Brain Sciences, Dartmouth College, Hanover, NH 03755, USA.

[8] Department of Biological Structure, University of Washington, Seattle, WA 98195, USA.

[9] Zanvyl Krieger Mind/Brain Institute, Johns Hopkins University, Baltimore, MD 21218, USA.

[10] Kavli Discovery Neuroscience Institute, Johns Hopkins University, Baltimore, MD 21218, USA.

[11] Department of Psychological and Brain Sciences, Johns Hopkins University, Baltimore, MD 21218, USA.

[12] Department of Neuroscience, Johns Hopkins University, Baltimore, MD 21218, USA.

[13] Department of Brain and Cognitive Sciences, Korea Advanced Institute of Science and Technology, Daejeon 34141, Republic of Korea.

[14] These authors contributed equally: Min Song, Eun Ju Shin.

* Correspondence to: daeyeol@jhu.edu; mwjung@kaist.ac.kr; sbpaik@kaist.ac.kr

Abstract

Timescales of temporally correlated neural activity vary systematically along the anatomical hierarchy of the primate cortex. Here, we found a similar hierarchical gradient of timescales in intrinsic as well as task-related cortical activities across monkeys, rats, and mice as they performed decision-making tasks, whereas the timescales of thalamic activity did not follow the anatomical hierarchy of their cortical counterparts. These findings suggest that the hierarchical ordering of cortical timescales may arise from intra-cortical recurrent connectivity rather than trans-thalamic projections, which reflects an evolutionary principle of cortical specialization shared across mammalian species.

Main

Cortical neurons show a wide range of persistency in stimulus-driven and other task-related activities, and display diverse patterns of temporal correlations and oscillations in their intrinsic activity even in the absence of task demands (Curtis and Lee, 2010; Wang, 2010). Despite the formidable complexity of the cortical network, its connectivity can be described parsimoniously by an anatomical hierarchy (Felleman and van Essen, 1991; Markov et al., 2014; Burt et al., 2018; Harris et al., 2019). Remarkably, the timescales of intrinsic neural activity in the primate cortex vary systematically with the anatomical hierarchy (Murray et al., 2014; Cirillo et al., 2018; Ito et al., 2020; Gao et al., 2020; Rossi-Pool et al., 2021; Manea et al., 2022). Furthermore, the timescales of persistent task-related activities follow a similar hierarchical ordering in the primate cortex (Spitmaan et al., 2020). These findings suggest that neuronal timescales can be considered as a general index of the functional organization across brain regions. Indeed, computational modeling and transcriptomics studies have suggested that variations in neuronal timescales can reflect the properties of intra-cortical circuits (Chaudhuri et al., 2015; Burt et al., 2018; Wengler et al., 2020; Gao et al., 2020). However, whether the hierarchical gradient of multiple timescales is a feature shared by cortical and subcortical areas and whether it is shared across different mammalian species remain unknown.

In the present study, we estimated four distinct types of timescales by employing an autoregressive time-series model, as previously described (Spitmaan et al., 2020) (**Fig. 1a**, see **Methods** for details). Two of them, referred to as intrinsic and seasonal timescales, quantify how quickly the strength of serially correlated neural activity decays within a trial and across trials, respectively. The other two, referred to as choice- and reward-memory timescales, correspond to how rapidly neural signals related to an animal's choice and reward decay. This analysis was applied to previously published data obtained from monkeys (866 neurons; Barraclough et al., 2004; Seo & Lee, 2007; Seo et al., 2009; Donahue et al., 2013), rats (4,972 neurons; Kim et al., 2009, 2013; Sul et al., 2010, 2011; Lee et al., 2012; Lee et al., 2017), and mice (12,691 neurons; Steinmetz et al., 2019) performing different choice tasks, namely a matching pennies task, dynamic foraging, and visual discrimination, respectively (**Figs. 1b**, **d**, and **f**; see **Methods** for details and **Supplementary Table 1** for information about the regions analyzed and corresponding abbreviations). We then examined how these timescales vary with the anatomical hierarchy, estimated based on the ratio of feedforward to feedback connections ("Hierarchy score", Felleman and Van Essen,

1991) in monkeys (Markov et al., 2014; Burt et al., 2018) and in mice (Harris et al., 2019). Given that mice and rats belong to the same subfamily, *Murinae* (Fabre et al., 2012; van den Heuvel et al., 2016; Scholtens et al., 2018), we used the hierarchy scores of mice as a proxy for those of rats.

First, we confirmed that cortical timescales increase with the anatomical hierarchy score similarly in monkeys, rats, and mice. As previously reported (Spitmaan et al., 2020), intrinsic, seasonal, choice-memory, and reward-memory timescales all increased with the anatomical hierarchy score in the monkey cortex (**Fig. 1c**). We also observed similar timescale-hierarchy score relationships across cortical areas in rats (**Fig, 1e**) and mice (**Fig. 1g**, black dots). This suggests that the hierarchical ordering of timescales is a universal feature of the cortical organization across mammalian species.

A high density of locally recurrent connections, which is a hallmark of cortical circuits (Shepherd, 2004), is thought to provide the biophysical basis for temporally extended cortical information processing, such as working memory and decision making (Wang, 2008; Murray et al., 2017). Alternatively, the hierarchical gradient of cortical timescales may be supported by, and hence present in, subcortical structures to which the cortex is closely connected. To test these scenarios, we used data from mice to assess whether timescales in various thalamic nuclei mirror the hierarchical gradient in their corresponding cortical counterparts (Harris et al., 2019). For each of the four timescales analyzed in this study, we found that the average timescale was shorter in the thalamus than in the cortex (**Fig. 1g,** red dots, rank-sum test; Intrinsic, $p = 2.2\times10^{-4}$; Seasonal, $p = 0.003$; Choice, $p = 0.004$; Reward, $p = 0.002$). Moreover, no significant correlation was found between the hierarchy score and any timescale in the thalamus (Pearson correlation coefficient, Intrinsic, $r = 0.509$, $p = 0.121$, Seasonal, $r = 0.376$, $p = 0.203$, Choice, $r = 0.078$, $p = 0.434$, Reward, $r = 0.422$, $p = 0.173$), and these correlations were significantly weaker than in the cortex (**Fig. 1g**, red dashed lines; **Supplementary Table 2**). This argues against the possibility that thalamic afferents are the major contributor to the hierarchical gradient of cortical timescales.

We then examined whether different timescales are correlated with one another. As previously shown in monkeys (**Fig. 2a**), seasonal, choice-memory, and reward-memory timescales were all found to be significantly correlated with intrinsic timescales across different neocortical areas in rats (**Fig. 2b**) and mice (**Fig. 2c**). This relationship did not change significantly when additional data from the striatum and hippocampus in rats (**Fig. 2b**,

green and pink dots) and the striatum and thalamus in mice were included (**Fig. 2c**, green and red dots; **Supplementary Table 3**). Thus, the relationship between intrinsic and other timescales is broadly consistent across the mammalian forebrain.

The fact that multiple timescales are correlated with one another across cortical areas suggests that they all result from a single mechanism, such as the strength of the local recurrent connectivity, which varies systematically across different brain areas. If this is the case, multiple timescales of *individual neurons* within the same brain area must be correlated with one another as well. Contrary to this prediction, however, intrinsic and other timescales of individual neurons were not significantly correlated within a given cortical area (Spitmaan et al., 2020), suggesting that different timescales can arise from multiple independent mechanisms. Similar to this previous finding in the primate cortex, we found that different timescales of individual neurons were not correlated with one another in any brain area of rats and mice ($p>0.05$, after Bonferroni correction for multiple comparisons; **Extended Data Fig. 1a**). To increase the reliability of the statistical analysis, we pooled the results from multiple brain areas after subtracting the average timescale for each area from those of individual neurons. Different timescales were not yet significantly correlated with one another, regardless of whether the results from all brain areas were combined or the areas within the neocortex, striatum, hippocampus, and thalamus were analyzed separately ($p>0.05$, after Bonferroni correction for multiple comparisons; **Extended Data Fig. 1b**). Therefore, hierarchical gradients of multiple timescales must be the result of multiple factors that vary independently within the population of neurons in each brain area and yet follow the same anatomical specialization across different brain areas.

In summary, we demonstrated that the hierarchical ordering of intrinsic, seasonal, and task-related timescales in the cortex is shared across mammalian species, which presumably reflects an evolutionarily conserved principle of cortical specialization. The fact that the timescales of neural activity in different thalamic nuclei did not simply mirror those in their cortical counterparts suggests that intra-cortical projections play a more important role in sculpting the gradient of cortical timescales than trans-thalamic projections (Saalmann & Kastner, 2011; Sherman & Guillery, 2011). Additional factors, such as variable temporal dynamics of synaptic transmission, may be also involved in the modulation of timescales, as suggested by studies of gene expression variations across

different cortical areas (Chaudhuri et al., 2015; Huntenburg et al., 2018; Demirtaş et al., 2019; Ito et al., 2020; Gao et al., 2020; Shafiei et al., 2020), raising the possibility that aberrant neuronal timescales may serve as a biomarker for psychiatric disorders (Watanabe et al., 2019; Wengler et al., 2020; Uscătescu et al., 2021; Wei et al., 2022). Given that timescales can be estimated from diverse ranges of neural data, from single-neuron recordings to non-invasive neuroimaging data, they can be used in future studies to gain a more complete understanding of the complex temporal dynamics of neural activity in humans and animals.

References

1. Curtis C.E. & Lee D. Beyond working memory: the role of persistent activity in decision making. Trends Cogn Sci. **14**, 216-222 (2010).
2. Wang X.J. Neurophysiological and computational principles of cortical rhythms in cognition. Physiol Rev. **90**, 1195-1268 (2010).
3. Felleman D.J. & Van Essen D.C. Distributed hierarchical processing in the primate cerebral cortex. Cereb. Cortex **1**, 1-47 (1991).
4. Markov N.T. et al. A weighted and directed interareal connectivity matrix for macaque cerebral cortex. Cereb. Cortex **24**, 17-36 (2014).
5. Burt J.B. et al. Hierarchy of transcriptomic specialization across human cortex captured by structural neuroimaging topography. Nat. Neurosci. **21**, 1251-1259 (2018).
6. Harris J.A. et al. Hierarchical organization of cortical and thalamic connectivity. Nature **575**, 195-202 (2019).
7. Murray J.D. et al. A hierarchy of intrinsic timescales across primate cortex. Nat. Neurosci. **17**, 1661-1663 (2014).
8. Cirillo R. et al. Neural Intrinsic Timescales in the Macaque Dorsal Premotor Cortex Predict the Strength of Spatial Response Coding. iScience **10**, 203-210 (2018).
9. Ito T. et al. A cortical hierarchy of localized and distributed processes revealed via dissociation of task activations, connectivity changes, and intrinsic timescales. Neuroimage **221**, 117141 (2020).
10. Gao R. et al. Neuronal timescales are functionally dynamic and shaped by cortical microarchitecture. Elife **9**, e61277 (2020).
11. Rossi-Pool R. et al. Invariant timescale hierarchy across the cortical somatosensory network. Proc. Natl. Acad. Sci U S A **118**, e2021843118 (2021).
12. Manea A.M.G. et al. Intrinsic timescales as an organizational principle of neural processing across the whole rhesus macaque brain. Elife **11**, e75540 (2022).
13. Spitmaan M. et al. Multiple timescales of neural dynamics and integration of task-relevant signals across cortex. Proc. Natl. Acad. Sci U S A **117**, 22522-22531 (2020).
14. Chaudhuri R. et al. A Large-Scale Circuit Mechanism for Hierarchical Dynamical Processing in the Primate Cortex. Neuron **88**, 419-431 (2015).
15. Wengler K. et al. Distinct hierarchical alterations of intrinsic neural timescales account for different manifestations of psychosis. Elife **9**, e56151 (2020).
16. Barraclough D.J. et al. Prefrontal cortex and decision making in a mixed-strategy game. Nat. Neurosci. **7**, 404-410 (2004).

17. Seo H. & Lee D. Temporal filtering of reward signals in the dorsal anterior cingulate cortex during a mixed-strategy game. J. Neurosci. **27**, 8366-8377 (2007).

18. Seo H. et al. Lateral intraparietal cortex and reinforcement learning during a mixed-strategy game. J. Neurosci. **29**, 7278-89 (2009).

19. Donahue C.H. et al. Cortical signals for rewarded actions and strategic exploration. Neuron **80**, 223-234 (2013).

20. Kim H. et al. Role of striatum in updating values of chosen actions. J. Neurosci. **29**, 14701-14712 (2009).

21. Kim H. et al. Signals for previous goal choice persist in the dorsomedial, but not dorsolateral striatum of rats. J. Neurosci. **33**, 52-63 (2013).

22. Sul J.H. et al. Distinct roles of rodent orbitofrontal and medial prefrontal cortex in decision making. Neuron **66**, 449-460 (2010).

23. Sul J.H. et al. Role of rodent secondary motor cortex in value-based action selection. Nat. Neurosci. **14**, 1202-1208 (2011).

24. Lee H. et al. Hippocampal neural correlates for values of experienced events. J. Neurosci. **32**, 15053-15065 (2012).

25. Lee S.H. et al. Neural Signals Related to Outcome Evaluation Are Stronger in CA1 than CA3. Front. Neural Circuits **7**, 11-40 (2017).

26. Steinmetz N.A. et al. Distributed coding of choice, action and engagement across the mouse brain. Nature **576**, 266-273 (2019).

27. Fabre P.H. et al. A glimpse on the pattern of rodent diversification: a phylogenetic approach. BMC Evol. Biol. **14**, 12-88 (2012).

28. Van den Heuvel M.P. et al. Comparative Connectomics. Trends Cogn. Sci. **20**, 345-361 (2016).

29. Scholtens L.H. et al. Cross-Species Evidence of Interplay Between Neural Connectivity at the Micro- and Macroscale of Connectome Organization in Human, Mouse, and Rat Brain. Brain Connect. **8**, 595-603 (2018).

30. Shepherd G.M.G. The Synaptic Organization of the Brain, 5th edn. (New York, 2004).

31. Wang X.J., Decision Making in Recurrent Neuronal Circuits, Neuron **60**, 215-234 (2008).

32. Murray J.D. et al. Working Memory and Decision-Making in a Frontoparietal Circuit Model. J Neurosci. **37**, 12167-12186 (2017).

33. Saalmann Y.B. & Kastner S. Cognitive and perceptual functions of the visual thalamus. Neuron **71**, 209-223 (2011).

34. Sherman S.M. & Guillery R.W. Distinct functions for direct and transthalamic corticocortical connections. J.

Neurophysiol. **106**, 1068-1077 (2011).

35. Huntenburg J.M. et al. Large-Scale Gradients in Human Cortical Organization. Trends Cogn. Sci. **22**, 21-31 (2018).
36. Demirtaş M. et al. Hierarchical Heterogeneity across Human Cortex Shapes Large-Scale Neural Dynamics. Neuron **101**, 1181-1194 (2019).
37. Shafiei G. et al. Topographic gradients of intrinsic dynamics across neocortex. Elife **9**, e62116 (2020).
38. Watanabe T. et al. Atypical intrinsic neural timescale in autism. Elife **8**, e42256 (2019).
39. Uscătescu L.C. et al. Reduced intrinsic neural timescales in schizophrenia along posterior parietal and occipital areas. NPJ Schizophr **7**, 55 (2021).
40. Wei Y. et al. Abnormal intrinsic neural timescale in Parkinson's disease. bioRxiv 508074 (2022).

Methods

Neural data

We analyzed single-neural activity collected previously from multiple brain regions of monkeys, rats, and mice. Specifically, we analyzed activity from four cortical areas in monkeys (Barraclough et al., 2004; Seo & Lee, 2007; Seo et al., 2009; Donahue et al., 2013) and from five cortical areas, three striatal subregions, and three hippocampal regions in rats (Kim et al., 2009, 2013; Sul et al., 2010, 2011; Lee et al., 2012; Lee et al., 2017). In addition, we used the dataset for mice publicly available at https://figshare.com/articles/dataset/Dataset_from_Steinmetz_et_al_2019/9598406 (Steinmetz et al., 2019), which includes neural activity recorded from eleven cortical areas, two striatal subregions, and seven thalamic nuclei. The numbers of neurons in each area from the three species are shown in **Supplementary Table 1**.

Behavioral task

Monkeys performed a matching pennies task (Barraclough et al., 2004; Seo & Lee, 2007; Seo et al., 2009; Donahue et al., 2013). The trial started with a yellow square presented at the center of the computer screen. After a delay of 0.5 seconds, two green disks were presented horizontally. The animal shifted its gaze towards one of the targets within 1 second and maintained its fixation for 0.5 seconds. Then, a red ring appeared around the target selected by the computer opponent, and the animal was rewarded only when it chose the same target as the computer. The computer opponent was programmed to predict the animal's choice based on the animal's previous choices and reward outcomes.

Rats performed dynamic foraging tasks (Kim et al., 2009, 2013; Sul et al., 2010, 2011; Lee et al., 2012; Lee et al., 2017). The rat was presented with two goal locations and allowed freely to choose one of them to receive a reward. One of the four reward probability pairs for left and right goal (left:right = 0.72:0.12, 0.63:0.21, 0.12:0.72, or 0.21:0.63) was used in each block with the number of trials in each block randomly determined.

Mice performed a visual discrimination task (Steinmetz et al., 2019). The trial began with visual stimuli presented on the left and right sides of the computer screen. After a delay of 0.5 to 1.2 seconds followed by an

auditory cue, the animal moved a stimulus of either side to the center of the screen by turning the wheel. If the animal chose the stimulus with higher contrast, it was rewarded. If the two stimuli were of equal contrast, the animal was rewarded with 50% probability for a left or right choice. If no stimuli were presented on the screen, the animal was rewarded only when it did not turn the wheel for 1.5 seconds following the auditory tone cue.

Hierarchy scores

The anatomical hierarchy scores for monkeys and mice used in this study were obtained from two prior studies (Brut et al., 2018; Harris et al., 2019), which are publicly available at https://balsa.wustl.edu/ and https://github.com/AllenInstitute/MouseBrainHierarchy, respectively. For the mice data, we used the hierarchy score calculated from the feedforward and feedback connections across the neocortical and thalamic areas, which are indicated as the 'CC+TC+CT iterated' scores in the result file 'hiearchy_summary_CreConf.xlsx', to compare the timescales from the areas in the neocortex and thalamic nuclei. For the rat data, the hierarchy scores from the mice were used.

Autoregressive model

Neural activity recorded from animals during the behavior tasks displays ongoing fluctuations within and across trials in addition to changes related to the animal's choices and their outcomes. In the present study, the timescales of intrinsic changes in the neural activity within a single trial and across multiple trials, referred to as 'intrinsic' and 'seasonal' timescales, respectively, were estimated using two separate groups of terms in a fifth-order autoregressive (AR) model (Spitmaan et al., 2020). In addition, we estimated the timescales of neural signals related to the animal's choice and its outcome by modeling them with the sum of the exponential functions with different time constants (**Fig. 1a**). To calculate these two timescales simultaneously, we used the same autoregressive model used in a previous study (Spitmaan et al., 2020), in which the timescales were estimated with a fitting algorithm to predict the current spike count of a neuron using the previous neural response and the history of the animal's choices and their outcomes in five previous trials. In this model, the spike counts in each time bin are predicted using the following model:

$$y(n,k) = \bar{y}(n) + A_U \times u + \sum_{i=1}^{5} a_{int}^{i} y(n-i,k) + \sum_{i=1}^{5} a_{sea}^{i} y(n,k-i) +$$
$$\bar{y}(n) \times A_{cho} \times \sum_{i=1}^{5} exp\left(-\frac{t_{cho}(n,k-i)}{\tau_{cho}}\right) \times cho(n,k-i) +$$
$$\bar{y}(n) \times A_{rew} \times \sum_{i=1}^{5} exp\left(-\frac{t_{rew}(n,k-i)}{\tau_{rew}}\right) \times rew(n,k-i)\,, \quad (1)$$

where $y(n,k)$ is the spike count in the nth bin (with a resolution of 50ms) of the kth trial and $\bar{y}(n)$ is a constant term for each bin, u is a set of behavioral terms (current choice, reward, and their interaction (choice $\times$ reward)), and a_{int}^{i} and a_{sea}^{i} are the corresponding coefficients for the intrinsic and seasonal AR components. These represent the intrinsic and seasonal fluctuations in the neural activity. $t_{cho}(n,k)$ and $t_{rew}(n,k)$ denote the time difference between the current time and the time when the choice was made and the reward was given in prior trials, respectively (with a resolution of 50ms). The free parameters of the model are the autoregressive coefficients for the intrinsic (a_{int}^{i}) and seasonal (a_{sea}^{i}) timescales; the amplitudes of the task-related, choice-memory, and reward-memory components denoted correspondingly by A_U, A_{cho}, and A_{rew}; and the timescales of the choice and reward signals indicated likewise by τ_{cho} and τ_{rew}. We estimated the time constants of choice- and reward-memory effects with individual exponential functions. For more details about the model, including the model selection method used to determine the statistical significance of the model parameters, we refer readers to Spitmaan et al. (2020).

The timescale of the intrinsic and seasonal fluctuations was calculated from the eigenvalues of five AR coefficients, as follows:

$$\tau = \max\left(-\frac{\Delta t}{\log(|\lambda|)}\right)$$
$$|F - \lambda I| = 0, F = \begin{pmatrix} a^1 & \cdots & a^5 \\ \vdots & \ddots & \vdots \\ 0 & \cdots & 0 \end{pmatrix}, \quad (2)$$

where Δt is the size of the time bin for each component (Δt= 50ms for the intrinsic timescale and the average trial length for the seasonal timescale).

To check for the possibility of overfitting due to high-order AR terms, we also performed the same analysis with a third-order AR model. We confirmed that the hierarchical gradients of the cortical timescales as reported in the main text were consistent regardless of the order of the AR model used (**Extended Data Fig. 2**).

Multiple-regression models

To examine the difference between the hierarchical gradient of each timescale in the cortex and thalamus, we used the following regression model (**Supplementary Table 2**):

$$\mathrm{T(n)} = a_0 + \mathrm{a_1 C(n)} + \mathrm{a_2 H(n)} + \mathrm{a_3 C(n)} \times \mathrm{H}(n) \ , \quad (3)$$

where $\mathrm{T(n)}$ is the population-averaged timescale in the nth brain area, $\mathrm{C(n)}$ is a dummy variable to indicate whether or not each area belongs to the cortex (that is, 0 and 1 for the thalamus and cortex, respectively), $\mathrm{H(n)}$ is the hierarchy score, and $\mathrm{C(n)} \times \mathrm{H(n)}$ is the interaction term. Thus, the null hypotheses that $a_3 = 0$ implies that that the strength of the correlation between the timescale and the hierarchy score is identical for both regions. Similarly, to test whether the correlations among multiple types of timescales differ for the neocortical and non-neocortical areas, we used the following regression model (**Supplementary Table 3**):

$$T(\mathrm{n}) = a_0 + \mathrm{a_1} C(\mathrm{n}) + \mathrm{a_2} \tau_{int}(\mathrm{n}) + \mathrm{a_3 C(n)} \times \tau_{int}(n) \ . \quad (4)$$

Data availability

All data used in this work are available at Zenodo (https://doi.org/10.5281/zenodo.7805638). Note that the data were obtained and curated from previously published data (see **Methods** for detailed information).

Code availability

MATLAB was used to perform the analysis during this work. The codes used in this work are referenced from publicly available codes at https://github.com/DartmouthCCNL/NeuroARMAX_LeeLabData (Spitmaan et al., 2020).

Acknowledgements

This work was supported by a grant from the National Research Foundation of Korea (NRF) funded by the Korean government (MSIT) (No. NRF-2022R1A2C3008991), by the Singularity Professor Research Project of KAIST (to S.P.), and by the Research Center Program of the Institute for Basic Science (IBS-R002-A1; to M.W.J.).

Author contributions

S.P., D.L., and M.W.J. designed and supervised the project. E.J.S. curated the data previously published or publicly available. M.S. analyzed the data. M.S. and E.J.S. drafted the paper and created the figures. S.P., D.L., and M.W.J. wrote the final version of the paper with input from all authors. All authors discussed and commented on the manuscript.

Competing interests

The authors declare no competing interests.

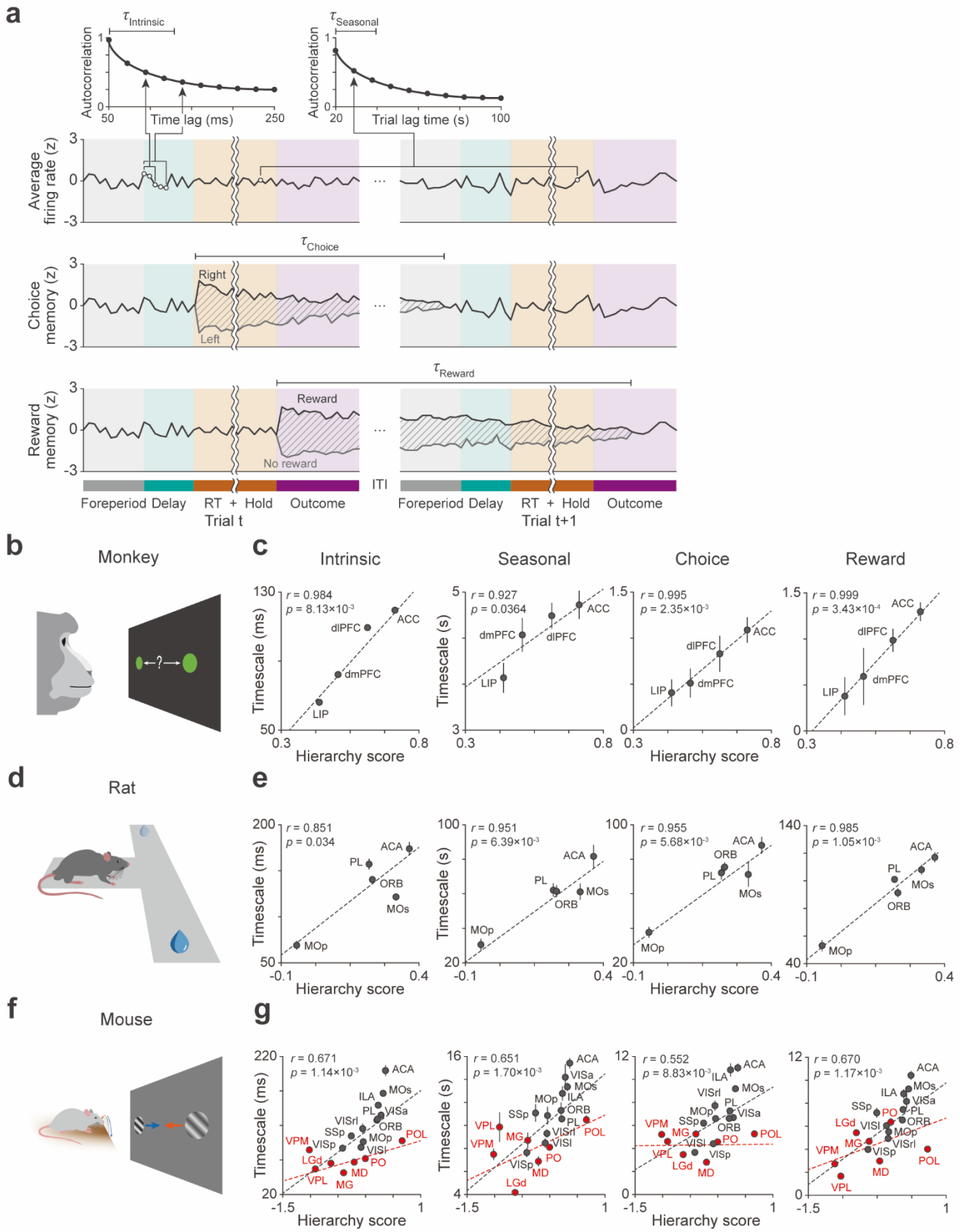

Fig. 1. Hierarchical ordering of multiple timescales in the neocortex: a. Estimations of multiple timescales with an autoregressive model are illustrated with imaginary neural data. Intrinsic and seasonal timescales estimate the change rate of correlated neural activity within a trial and across trials, respectively, whereas choice- and reward-memory timescales quantify the decay of neural signals related to the animal's choice and reward outcome, respectively. **b.** Matching pennies task for monkeys. **c.** Correlation between the timescales of the neural activity and anatomical hierarchy score in monkeys. Each dot indicates a population-averaged timescale within each area, and the dashed lines represent linear regressions of the data. **d.** Dynamic foraging task for rats. **e.** Correlation between the timescales and hierarchy score in rats. **f.** Visual discrimination task for mice. **g.** Correlation between the timescales and hierarchy score in mice. Black and red dots (dashed lines) represent data (regression lines) from the neocortex and thalamus, respectively. The Pearson correlation coefficients *r* and the *p* values for the data pooled from all areas in each species are shown in **Figs. 1c**, **e**, and **g**. Error bars show the standard error of the median.

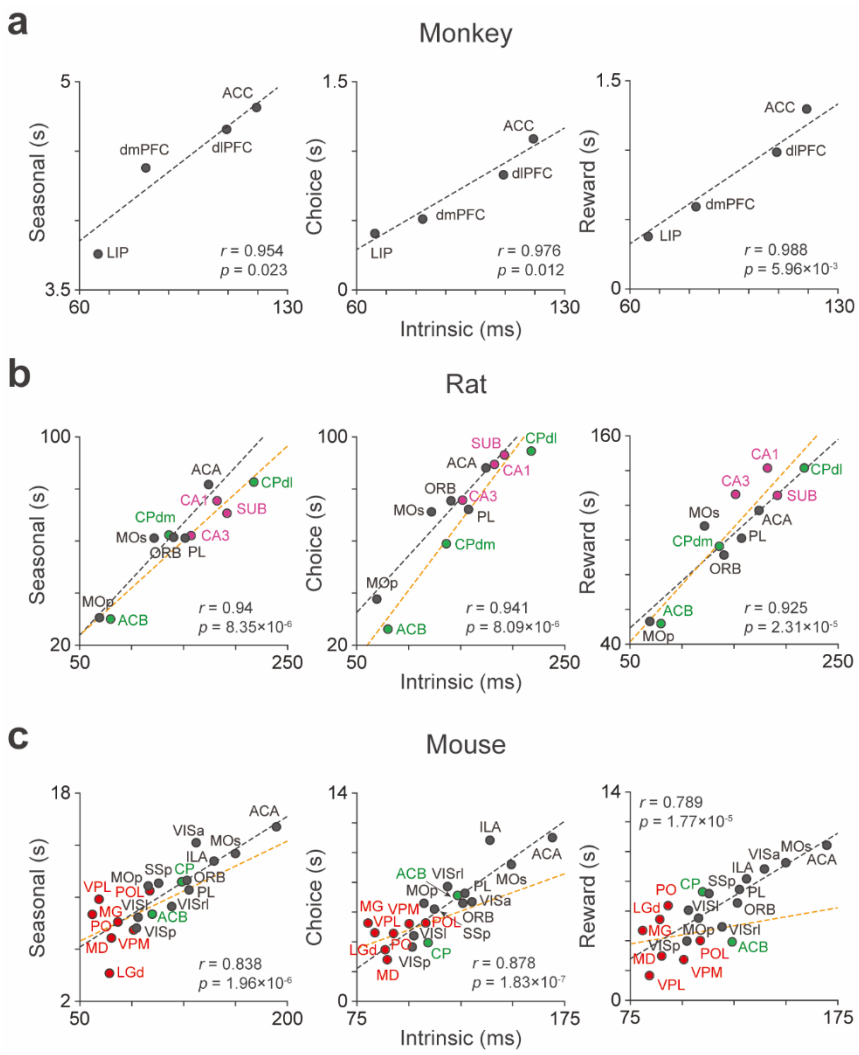

Fig. 2. Correlations between different timescales: a-c. Correlation between the intrinsic timescale and the seasonal, choice-memory, and reward-memory timescales in monkeys (a), rats (b), and mice (c), respectively. Population-averaged timescales are shown for the neocortex (black), striatum (green), hippocampus (pink), and thalamus (red). Dashed lines show the regression outcomes for the results from the neocortical (black) and non-neocortical (orange) areas. The Pearson correlation coefficients *r* and the *p* values for the data pooled from all areas are shown. When the data from non-neocortical areas were analyzed separately, the intrinsic timescales were significantly correlated with the other timescales in rats (Pearson correlation coefficient, Seasonal, r = 0.966, p = 0.002, Choice, r = 0.934, p = 0.007, Reward, r = 0.974, p = 0.001), but not in mice (Pearson correlation coefficient, Seasonal, r = 0.512, p = 0.159, Choice, r = 0.567, p = 0.111, Reward, r = 0.19, p = 0.625), presumably reflecting the properties of the thalamic nuclei.

Species	Abbreviation	Full name	Number of neurons	Number of animals
Monkey	ACC	Anterior cingulate cortex	154	2
	dlPFC	Dorsolateral prefrontal cortex	322	5
	dmPFC	Dorsomedial prefrontal cortex	185	2
	LIP	Lateral intraparietal cortex	205	3
	Total		866	6
Rat	ACA	Anterior cingulate area	679	5
	ORB	Orbital area	1148	3
	PL	Prelimbic area	854	6
	MOp	Primary motor area	227	3
	MOs	Secondary motor area	411	3
	CPdm	Dorsomedial caudoputamen	414	6
	CPdl	Dorsolateral caudoputamen	129	3
	ACB	Nucleus accumbens	165	3
	CA1	Field CA1 (Cornu Ammonis 1)	599	9
	CA3	Field CA3 (Cornu Ammonis 3)	231	4
	SUB	Subiculum	115	3
	Total		4972	27
Mouse	ACA	Anterior cingulate area	841	8
	ORB	Orbital area	660	4
	PL	Prelimbic area	863	7
	ILA	Infralimbic area	411	3
	MOp	Primary motor area	793	3
	MOs	Secondary motor area	1743	9
	SSp	Primary somatosensory area	515	4
	VISa	Anterior visual area	340	4
	VISl	Lateral visual area	434	2
	VISp	Primary visual area	1118	8
	VISrl	Rostrolateral visual area	286	2
	CP	Caudoputamen	1215	5
	ACB	Nucleus accumbens	337	3
	LGd	Dorsal part of the lateral geniculate complex	882	5
	POL	Posterior limiting nucleus of the thalamus	215	3
	MD	Mediodorsal nucleus of the thalamus	397	3
	VPL	Ventral posterolateral nucleus of the thalamus	301	3
	PO	Posterior complex of the thalamus	692	4
	VPM	Ventral posteromedial nucleus of the thalamus	353	2
	MG	Medial geniculate complex of the thalamus	295	2
	Total		12691	10

Supplementary Table 1. Brain regions analyzed in each species. The number of neurons and animals obtained from each region and species used for analysis are shown.

Timescales	Intercept	Region	Hierarchy score	Region x Hierarchy score
Intrinsic	20.8 (6.53×10^{-12})	−4.30 (7.27×10^{-4})	4.97 (2.07×10^{-4})	−3.78 (2.03×10^{-3})
Seasonal	20.1 (1.02×10^{-11})	−2.52 (0.025)	3.60 (2.89×10^{-3})	−2.58 (0.022)
Choice	15.2 (4.18×10^{-10})	−2.93 (0.011)	3.87 (1.7×10^{-3})	−3.3 (5.31×10^{-3})
Reward	15.7 (2.76×10^{-10})	−3.03 (8.94×10^{-3})	3.69 (2.45×10^{-3})	−2.59 (0.022)

Supplementary Table 2. Results from the regression model to test the differences in the correlations between the timescales for the neocortex and thalamic nuclei in mice. Results of t-statistics (p) are shown for different regressors in the regression model given by Equation (3) (see **Methods** for details).

Animal	Timescales	Intercept	Region	Intrinsic	Region x Intrinsic
Rat	**Seasonal**	0.226 (0.828)	0.248 (0.811)	5.93 (5.82×10^{-4})	−0.745 (0.481)
	Choice	0.956 (0.371)	−0.448 (0.667)	3.23 (0.015)	0.563 (0.591)
	Reward	0.982 (0.387)	−1.46 (0.188)	5.31 (1.11×10^{-3})	0.87 (0.413)
Mouse	**Seasonal**	1.92 (0.073)	0.4 (0.69)	4.23 (6.42×10^{-4})	−0.529 (0.6)
	Choice	−0.2 (0.843)	1.32 (0.206)	5.82 (2.62×10^{-5})	−1.48 (0.158)
	Reward	0.4 (0.695)	1.02 (0.324)	3.91 (1.25×10^{-3})	−1.44 (0.169)

Supplementary Table 3. Results from the regression model used to test the differences in the relationships between the intrinsic and other timescales between the neocortical and non-neocortical areas. Results of t-statistics (p) are shown for different regressors in the regression model given by Equation (4) (see **Methods** for details). Non-neocortical areas refer to the striatum and hippocampus for rats, and the striatum and thalamus for mice.

Extended data

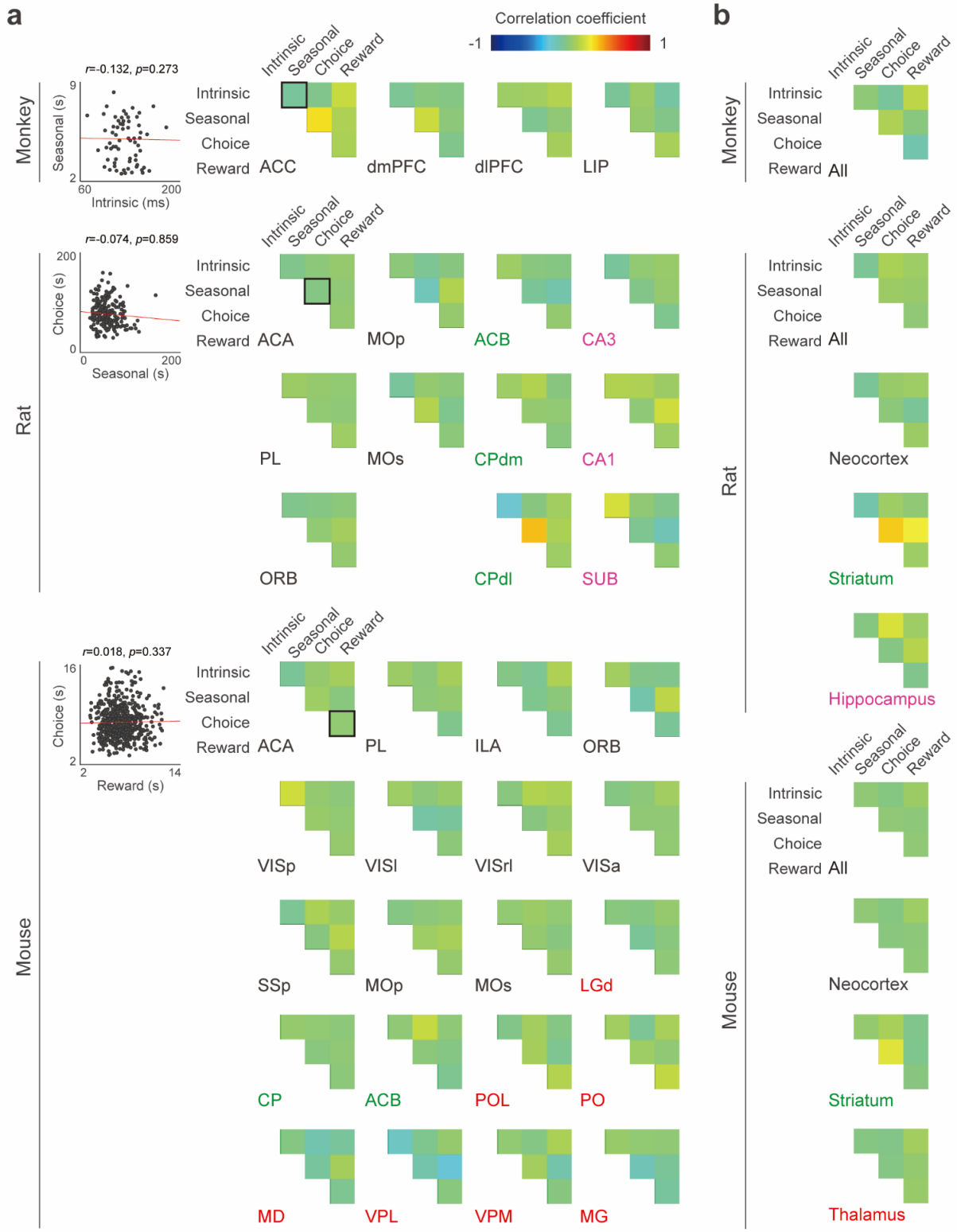

Extended Data Fig. 1. Lack of a correlation between multiple timescales across individual neurons. a. Pearson correlation coefficients between all pairs of different timescales measured from individual neurons in different brain areas of monkeys, rats, and mice. In each species, the relationship between different timescales across neurons is shown for the anterior cingulate cortex (ACC or ACA), as indicated by the black box in the correlation matrix. **b.** Corresponding results for the residual timescales combined for all brain areas tested in the present study. None of these correlations was statistically significant (p>0.05, after Bonferroni correction for multiple comparisons).

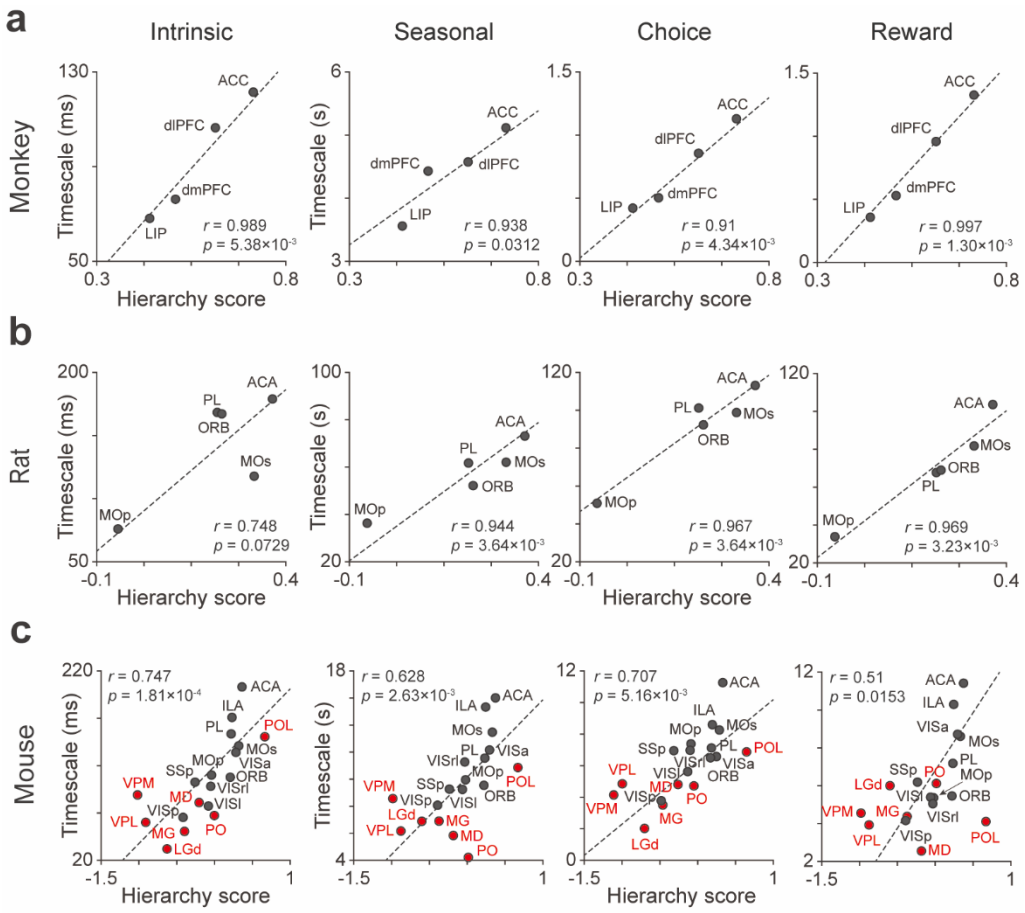

Extended Data Fig. 2. Correlation between the timescales of the neural activity and anatomical hierarchy score estimated with a third-order autoregressive model. a-c. Correlation between the timescales of the neural activity and anatomical hierarchy score in monkeys (a), rats (b), and mice (c), respectively. The format here is identical to that in **Figures 1c**, **e**, and **g**.